8-20-2010

EBC Development for Hot-Pressed Y_2O_3/Al_2O_3 Doped Silicon Nitride Ceramics

Sivakumar Ramasamy
Cleveland State University

Surendra N. Tewari
Cleveland State University

Kang N. Lee
Rolls-Royce Corporation

Ramakrishna T. Bhatt
NASA Glenn Research Center

Dennis S. Fox
NASA Glenn Research Center

Original Citation

Ramasamy, S., Tewari, S., Lee, K., Bhatt, R., , & Fox, D. (2010). EBC development for hot-pressed EBC development for hot-pressed Y2O3/Al2O3 doped silicon nitride ceramics doped silicon nitride ceramics. Materials Science & Engineering A, 527(21-22), 5492-5498. doi:10.1016/j.msea.2010.05.067

EBC development for hot-pressed Y_2O_3/Al_2O_3 doped silicon nitride ceramics

Sivakumar Ramasamy[a,*], Surendra N. Tewari[a], Kang N. Lee[b], Ramakrishna T. Bhatt[c], Dennis S. Fox[c]

[a] Cleveland State University, Chemical and Biomedical Engineering, 2121 Euclid Avenue, Cleveland, OH, USA
[b] Rolls-Royce Corporation, P.O. Box 420, Indianapolis, IN, USA
[c] NASA Glenn Research Center, 21000 Brook Park Rd., Cleveland, OH, USA

1. Introduction

Silicon nitride is a promising candidate material for use as hot-section engine component for gas turbines and internal combustion engines because of its low thermal expansion coefficient and high temperature strength, toughness and creep resistance [1–7]. Additives such as Y_2O_3, Al_2O_3, Lu_2O_3 and other rare-earth oxides have been used to sinter silicon nitride powder in order to create monolithic silicon nitride components [2–4,8–10]. It has been shown that in an oxidizing environment migration of these additives from the grain boundary regions to the surface [4,11] adversely affects the mechanical properties and oxidation resistance of silicon nitride. Silicon nitride undergoes parabolic oxidation to form a thin protective layer of silica (SiO_2) on its surface that prevents its further oxidation in dry oxygen environment. However, in the presence of water vapor the silica formed is converted into volatile silicon hydroxide species ($Si(OH)_4$) via the following reactions [12–16].

$$Si_3N_4(s) + 6H_2O(g) = 3SiO_2(s) + 2N_2(g) + 6H_2(g) \quad (1)$$

$$SiO_2(s) + 2H_2O(g) = Si(OH)_4(g) \quad (2)$$

The simultaneous oxidation of silicon nitride and volatilization of SiO_2 scale leads to rapid surface recession of the material. For instance, in micro-turbine environment, silicon nitride surface recedes at the rate of 1 mg/cm^2 hour [17]. Since water vapor is a byproduct of the hydrocarbon combustion, use of silicon nitride as advanced gas turbine engine components is only possible if suitable environmental barrier coatings (EBCs) can be developed that can inhibit moisture transport to the substrate.

Monolith mullite and mullite based refractory oxides have been proposed as EBCs for silicon nitride substrates in most studies due to their excellent environmental stability [17–20]. And, among different techniques available, atmospheric plasma spraying (APS) [18,19] and chemical vapor deposition (CVD) [20,21] are widely employed to deposit EBCs on Si_3N_4 substrates. But, these techniques are time consuming and expensive. In particular, APS is a line-of-sight process which does not allow coating of complex shaped components, especially those containing internal cooling channels. In addition, silicon nitride components require surface roughening by chemical etching or grit-blasting in order to promote mechanical interlocking of the plasma-sprayed coating with the substrate. This adversely affects the toughness of the substrates; for example for silicon nitride components it has been observed to cause more than 50% strength debit at room temperature and 15% debit at high temperatures [22]. Hence, a non-line-of-sight process needs to be developed to deposit EBCs on complex shaped components without adversely affecting the substrate fracture strength.

Slurry based dip coating is a non-line-of-sight process allowing coating of complex shaped components with ease and it is in-expensive. It also facilitates developing strain tolerant microporous bond coat that can chemically adhere to the substrate without any need for surface roughening. Slurry based coatings have been examined for EBC on Si_3N_4 substrates [17,23–26]. Pur-

Table 1
Materials used in this study and their co-efficient of thermal expansion.

Material	Co-efficient of thermal expansion, CTE ($\times 10^{-6}$/°C)
Silicon nitride (Si_3N_4)	3–4 [20]
Mullite	5–6 [20]
Gadolinium silicate (Gd_2SiO_5)	10.1 [27]
Lutetium silicate (Lu_2SiO_5)	7.9 [27]
Erbium silicate (Er_2SiO_5)	5–7 [20]
Hafnium silicate ($HfSiO_4$)	3.6 [28]

pose of this study was to explore slurry based coatings for EBC applications on hot pressed silicon nitride samples containing 2 wt.% alumina and 5 wt.% yttria sintering additives. The usefulness of deposited EBCs was evaluated by thermal cycling performance of EBC coated silicon nitride coupons in simulated combustion environments and the results are discussed in this study.

2. Experimental procedure

2.1. Materials and processing

Multilayer EBCs were applied by dip coating process onto hot-pressed Y_2O_3/Al_2O_3 doped Si_3N_4 coupons (Ram Bhatt, NASA Glenn Research Center, Cleveland, USA) of dimensions 24.9 mm × 3.2 mm × 2.3 mm. The following slurry formulations were studied to explore a range of sintering temperatures for the EBC coatings.

(a) A low melting temperature formulation based on 45% SiO_2–34% Y_2O_3–21% Al_2O_3 (d_{50}: 0.9 μm, Praxair Surface Technologies, USA). This composition is similar to the yttria-alumina-silica glass system (YAS-1) investigated by Hyatt and Day [26] which had glass transformation and softening temperatures, 889 °C and 933 °C, respectively.
(b) Intermediate melting temperature formulation based on boron-oxide containing (about 5 wt.% B_2O_3) and boron-oxide free 88 wt.% mullite–12 wt.% Gd_2SiO_5.
(c) High melting temperature formulation based on 94 wt.% mullite–6 wt.% rare earth silicates (Gd_2SiO_5, Lu_2SiO_5, Er_2SiO_5, and $HfSiO_4$).
(d) Mullite sol based EBC containing mullite powders.

The starting materials and their particle sizes considered in this study are as follows:

(a) Mullite (d_{72}: 3 μm, Baikowski International Corporation, USA).
(b) Rare-earth-silicates (Praxair Surface Technologies, USA): Gadolinium silicate (Gd_2SiO_5, d_{50}: 0.9 μm), lutetium silicate (Lu_2SiO_5, d_{50}: 1 μm), erbium silicate (Er_2SiO_5, d_{50}: 0.8 μm) and hafnium silicate ($HfSiO_4$, d_{50}: 0.7 μm). Table 1 summarizes the materials and their co-efficient of thermal expansion investigated in this study.
(c) For sol-based mullite slurry, alumina sol (Nanodur) and silica sol (tetramethyl-ammonium silicate $(CH_3)_4NOH{\cdot}2SiO_2$)) were purchased from Alfa Aesar, USA.

Our earlier results [29–31] demonstrated that mullite-based slurries for ceramic substrates can be prepared by blending mullite and rare-earth silicate powders with polyvinyl butyral (PVB) as a binder, phosphate ester (PE) as a dispersant, and ethyl alcohol as the solvent. In this study, powder mixtures as described above were milled by planetary milling for 30 min to enhance molecular level mixing between starting materials before their addition to the ethanol based solution containing 4 wt.% of PVB and 0.6 wt.% of PE. The slurry with solid-liquid ratio of 1:2 was magnetically stirred and mixed for 12 h before being used to coat silicon nitride coupons. Multilayer mullite or mullite-rare earth silicate EBCs were deposited on Si_3N_4 coupons for 30 s through an indigenously developed coating set-up that utilized controlled sample dip and withdrawal rates, and also the rotation speeds to drain-off the excess slurry from the sample surface. The coated coupons after vacuum drying at room temperature were air or vacuum sintered at temperatures between 1375 °C and 1475 °C.

In addition to the above described PVB-PE-alcohol route, sol-based mullite slurry was also examined for EBC application in this study. Alumina sol and silica sol (3:2 ratio) were first thoroughly mixed using a high intensity ultrasonic mixer and then mullite powder was added to this sol-mixture in a 1:1 weight ratio to prepare the slurry. Since PVB and PE were not added in the sol-based slurry it was expected that the sintered EBC coatings using this approach would have smaller and more finely distributed pores than the organic solvent based coating having PVB, PE and alcohol. In addition, since a large fraction of mullite was to be formed in situ via reaction of the silica and alumina sols at high temperatures, faster densification kinetics was also expected for the sol-based coatings. Using this slurry, multilayer coatings were applied on Si_3N_4 coupons by the aforementioned dip coating procedure and sintered in air up to 1430 °C for 3 h.

2.2. Evaluation and characterization

The durability of EBCs on Si_3N_4 coupons was evaluated by exposing coated samples to thermal cycling in a simulated combustion environment using an automated thermal cycling furnace. Thermal cycling was conducted between 1350 °C and room temperature (RT) in 90% H_2O–10% O_2 atmosphere with a flow rate of 2.2 cm/s at 1 atm using an automated thermal cycling furnace described in Ref. [32]. Each thermal cycle consisted of 75 min, with the samples being in the hot zone (1350 °C) for 1 h followed by rapid cooling to RT (cold zone), and staying at RT for 15 min. Coated samples were examined after sintering in air and also after thermal cycling in moisture by optical and scanning electron microscopy (SEM, AMRAY 1820, USA).

For the sol-based coatings, an XRD analysis using semi-quantitative relative intensity ratio (RIR) was used to determine the extent of conversion of the alumina and silica sols in the mixture to mullite after 5 h sintering in air at temperatures varying from 1300 °C to 1375 °C. Four point bend strength tests were also performed on coated coupons to determine the room temperature strength debit, if any, with respect to un-coated Si_3N_4 monoliths.

3. Results and discussion

3.1. EBC coatings for Si_3N_4

3.1.1. Low melting temperature formulation (45% SiO_2–34 wt.% Y_2O_3–21 wt.% Al_2O_3)

Fig. 1(a) and (b) shows the low and high magnification optical images of Si_3N_4 coupons coated with a 45 wt.% SiO_2–34 wt.% Y_2O_3–21 wt.% Al_2O_3 slurry and sintered in air atmosphere at 1375 °C for 3 h. From the figure, it is evident that there was a good coverage of coating on the substrate; however, extensive bubbles were formed after sintering. Further, high magnification image reveals that there is glass formation on Si_3N_4 surface after air sintering. Thus, this slurry is considered to be unsuitable as an EBC for Y_2O_3 doped Si_3N_4 substrates.

3.1.2. Intermediate melting temperature formulation (mullite/Gd_2SiO_5 (88/12 wt.%))

3.1.2.1. B_2O_3 (5 wt.%) containing. Fig. 2(a)–(c) shows the optical images of Y_2O_3/Al_2O_3 doped Si_3N_4 coupons coated with

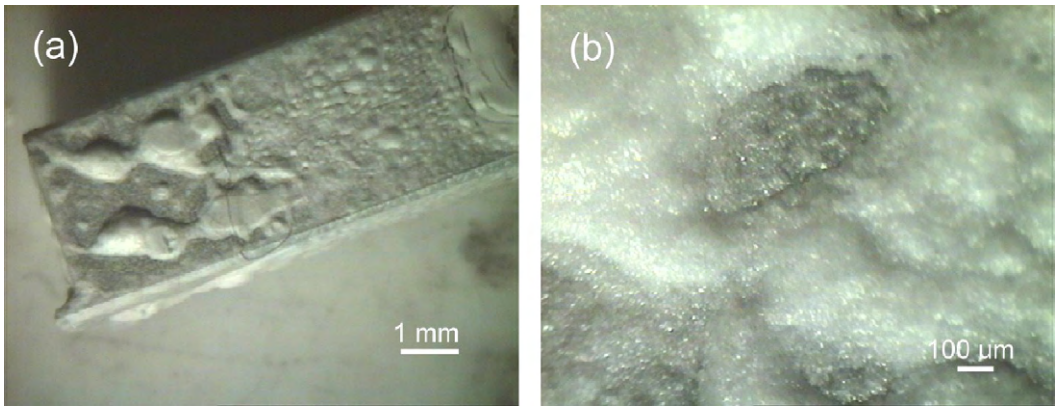

Fig. 1. Low and high magnification optical images of Y_2O_3/Al_2O_3 doped Si_3N_4 coupons coated with low melting point 45 wt.% SiO_2–34 wt.% Y_2O_3–21 wt.% Al_2O_3 slurry showing extensive bubble formation after sintering in air atmosphere at 1375 °C for 3 h.

mullite/Gd_2SiO_5/B_2O_3 (83.5/11.5/5 wt.%) EBC and sintered in air for 3 h at 1375 °C, 1400 °C and 1450 °C, respectively. A small amount of boron oxide (B_2O_3, 5 wt.%) included in the slurry was to investigate the effect of sintering aid addition. As shown in Fig. 2, smooth and good coating integrity was present after sintering at 1375 °C (Fig. 2(a)). On the other hand, when the B_2O_3 containing mullite/Gd_2SiO_5 coatings were sintered at 1400 °C, hair line cracks were initiated on the surface as shown in Fig. 2(b). With still increased sintering temperature at 1450 °C, bubbles were formed on surface (Fig. 2(c)), which makes these mullite/Gd_2SiO_5/B_2O_3 EBCs unacceptable for temperatures more than 1400 °C. Four point bend strength tests at room temperature were evaluated for two mullite/Gd_2SiO_5/B_2O_3 coated coupons that were sintered at 1375 °C and the results showed fracture strength values of 532 MPa and 758 MPa. This compares well with the room temperature fracture strength value of uncoated Si_3N_4 samples, 570 ± 70 MPa [22].

3.1.2.2. B_2O_3 free. Mullite/Gd_2SiO_5 (88/12 wt.%) EBC was coated on Y_2O_3/Al_2O_3 doped Si_3N_4 coupons and Fig. 3(a) and (b) shows the optical and the SEM images after sintering at 1400 °C in air for 3 h. Since the slurry did not contain sintering additive (B_2O_3), its sintering temperature was expected to be slightly higher than that for the B_2O_3 containing slurry described above. The optical image of mullite/Gd_2SiO_5 EBC (Fig. 3(a)) revealed that there was an excellent coating integrity and adherence to the substrate even when sintered in air atmosphere, with minimal surface micro-cracks.

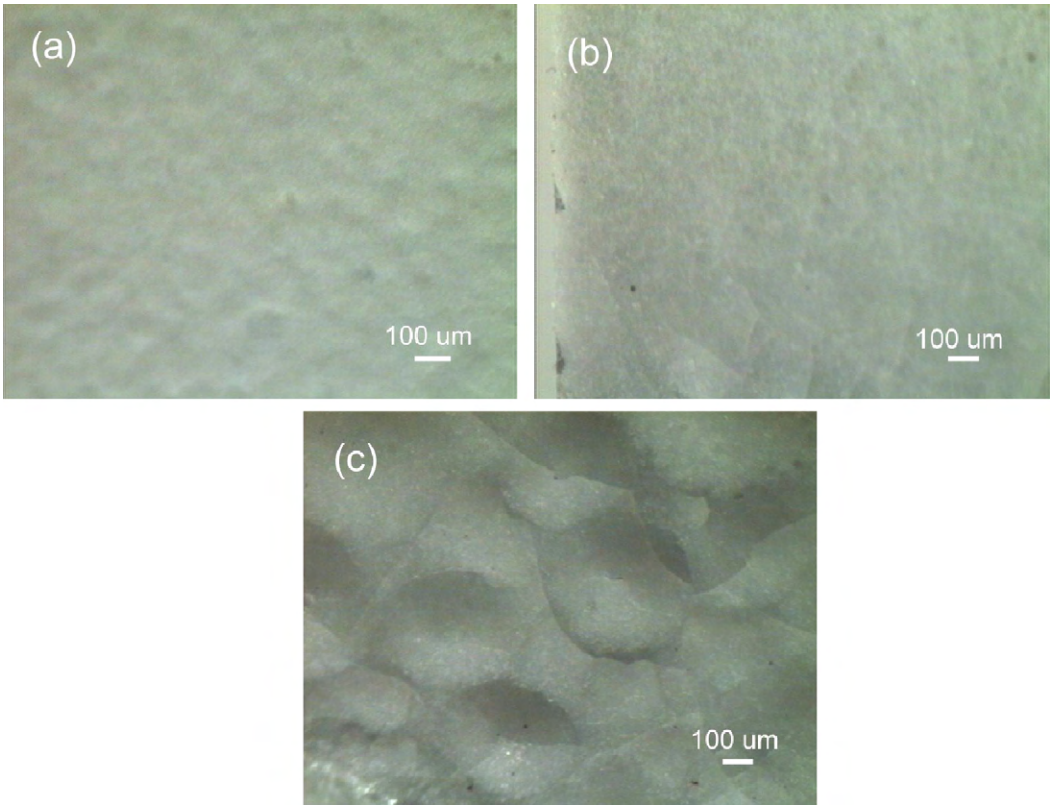

Fig. 2. Optical images of Y_2O_3/Al_2O_3 doped Si_3N_4 coupons coated with intermediate melting point mullite/Gd_2SiO_5 (83.5/11.5 wt.%) slurry containing 5 wt.% of B_2O_3 and air sintered at: (a) 1375 °C, (b) 1400 °C, and (c) 1450 °C, respectively for 3 h. The coating showed surface cracks and bubble formation when sintered at 1400 °C and 1450 °C, respectively.

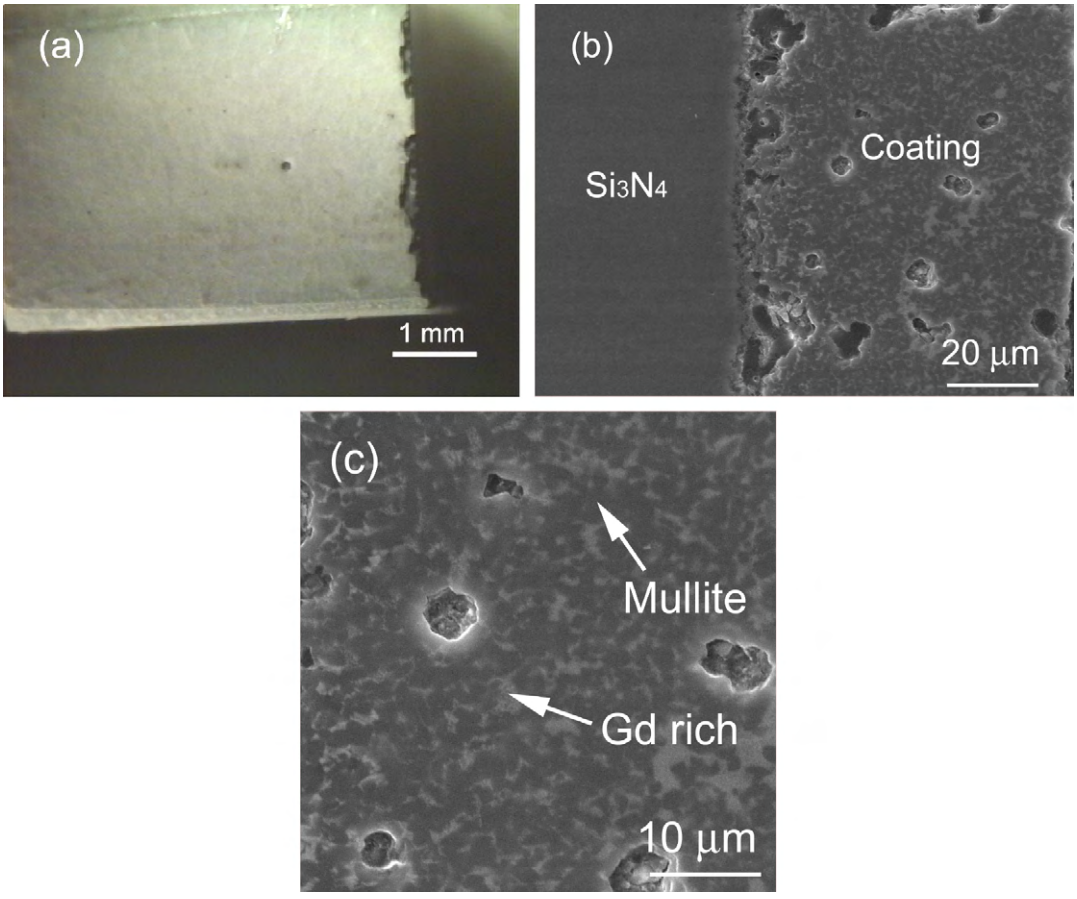

Fig. 3. Y_2O_3/Al_2O_3 Si_3N_4 coupon coated with intermediate melting point mullite/Gd_2SiO_5 (88/12 wt.%) slurry and air sintered at 1400 °C. (a) Optical image that indicates a good coating coverage over substrate without surface bubbling after sintering, (b) SEM cross-section depicting an uniform adhesion of coating to substrate, and (c) high magnification SEM view of coating consisting mullite particles imbedded in gadolinium (rich) glassy phase.

Fig. 3(b) shows a SEM cross-sectional view of mullite/Gd_2SiO_5 EBC coated Si_3N_4 coupons. From the figure, it can be seen that the coating densified well after sintering at 1400 °C. Porosities were observed in the sintered coating but they did not seem to be interconnected. Attempt to further densify the coating by sintering at 1415 °C and higher temperature was futile, because it resulted in bubble formation and coat de-bonding.

A higher magnification SEM view of the coating sintered at 1400 °C shows it to be having a dual phase microstructure with the mullite particles imbedded in a gadolinium (rich) glassy phase (Fig. 3(c)). The room temperature fracture strength values of two mullite/Gd_2SiO_5 EBC coated Si_3N_4 coupons measured were 688 MPa and 632 MPa (as compared with uncoated Si_3N_4: 570 ± 70 MPa).

3.1.3. *High melting temperature formulations (mullite/rare earth silicates (94/6 wt.%), Gd_2SiO_5, Lu_2SiO_5, Er_2SiO_5, and $HfSiO_4$)*

The maximum safe sintering temperature to achieve coat-densification without gaseous bubble formation can be increased by increasing the mullite content of the slurry. The mullite/Gd_2SiO_5 (94/6 wt.%) EBC for example, sintered up to 1415 °C did not show apparent surface bubble formation as shown in the low-magnification optical view in Fig. 4(a). However, the SEM cross-sectional view confirmed a dense coating with severe coating delamination (Fig. 4(b)). Similarly, coatings of mullite slurries containing 6 wt.% lutetium silicate (Lu_2SiO_5) or 6 wt.% hafnium silicate ($HfSiO_4$), (not shown in figures) exhibited the same behavior as mullite/Gd_2SiO_5 (94/6 wt.%) coating. In addition after sintering at 1430 °C, they all showed extensive bubbling just below the top dense layer, typically shown for a mullite/erbium silicate (Er_2SiO_5) (94/6 wt.%) EBC in Fig. 4(c).

3.1.4. *Mullite sol based slurry containing only mullite particles*

Mullite sol prepared by mixing the alumina sol and tetramethylammonium silicate to yield 3:2 alumina-silica mullite was subsequently mixed with mullite powder to prepare the mullite based slurry without sintering additive, as described in Ref. [30]. X-ray diffraction results [30] from the mullite powder/mullite sol slurry sintered at 1375 °C for 5 h indicated about 92% mullite and the rest crystobalite and α-alumina. As shown in Fig. 5(a), the substrate/coating interface showed good bonding at 1400 °C, but the coating was still porous. Attempts to sinter the coating at a higher temperature of 1430 °C were futile, because as shown in Fig. 5(b), large bubbles formed at the interface and lifted the coating off from the substrate causing severe delamination.

3.2. *Thermal cycling of the optimum EBC coating (mullite/Gd_2SiO_5 (88/12 wt.%)) in moisture environment*

Among all studied EBCs, the mullite/Gd_2SiO_5 (88/12 wt.%) EBC (Fig. 3(b)) revealed a dense coating with excellent coating integrity and adherence to Si_3N_4 substrate after sintering. Therefore, the durability of these coated coupons was evaluated through thermal cycling in moisture containing combustion environment. Fig. 6 exhibits low magnification (montage) cross-sectional SEM view of the mullite/Gd_2SiO_5 (88/12 wt.%) EBC coated Si_3N_4 coupon after 100 thermal cycles in 90% H_2O vapor-balance O_2 environment between 1350 °C and room temperature (1 h hot and 15 min cold).

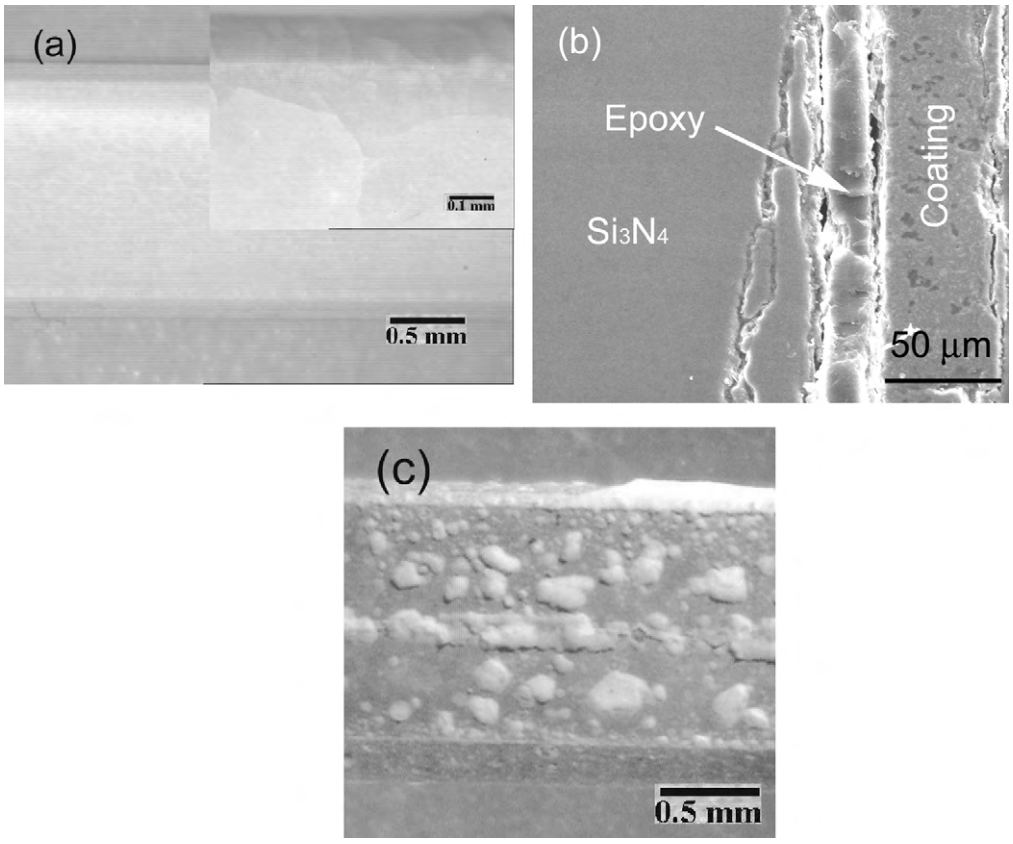

Fig. 4. Y_2O_3/Al_2O_3 Si_3N_4 coupon coated with high melting point slurry. (a) Optical image of mullite/Gd_2SiO_5 (94/6 wt.%) slurry coating and air sintered at 1415 °C for 3 h (inset shows high magnification view), (b) SEM cross-section indicating coating delamination from Si_3N_4 substrate and (c) substantial surface bubbling on Si_3N_4 substrate when mullite/Er_2SiO_5 (88/12 wt.%) slurry coated and air sintered to 1430 °C for 3 h.

There was a noticeable densification of the EBC during thermal cycling because of the 100 h exposure at 1350 °C (compare Fig. 3(b) with Fig. 6). Thermal cycling also produced hairline cracks along substrate/coating interface, which were presumably caused by the stresses generated from coefficients of thermal expansion (CTE) mismatch between Si_3N_4 and coating constituents as shown in Table 1. But the more serious problem is the formation of large, elongated and almost interconnected pores in the coating adjacent to the interface which leads to coating spallation. Void consolidation during densification may account for some of the void accumulation at substrate/coating interface. But the volume fraction of the voids in thermal cycled samples is much too large and must be associated with the moisture induced oxidation, and formation of volatile $Si(OH)_4$ and nitrogen oxide. Since the coating

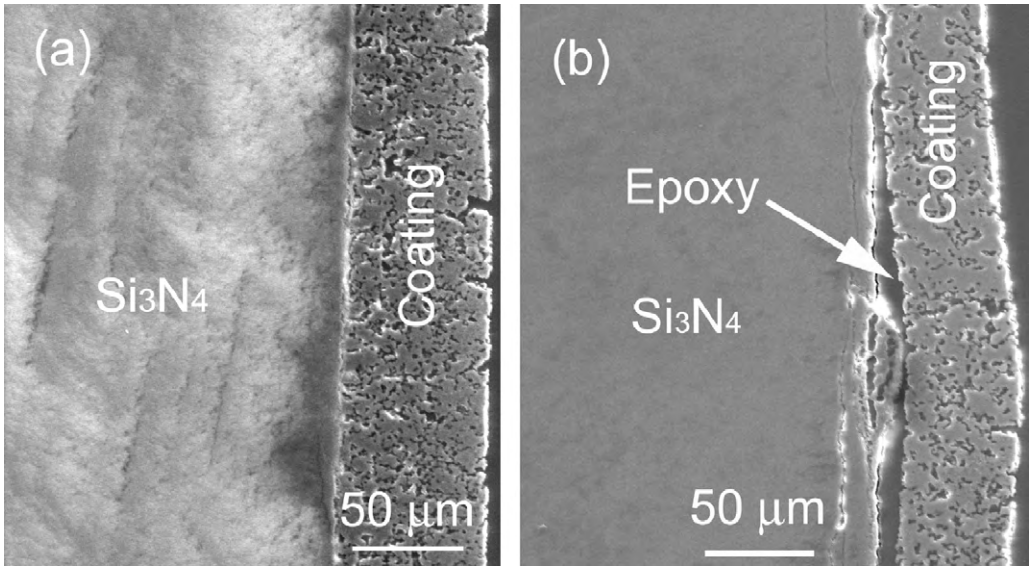

Fig. 5. SEM cross-sectional views of mullite powder/mullite sol (50/50 wt.%) slurry coatings on Y_2O_3/Al_2O_3 Si_3N_4 doped Si_3N_4 coupon and air sintered to (a) 1415 °C for 3 h, where the porous coating adhered well to substrate, and (b) 1430 °C for 3 h, where the coating delaminated from substrate.

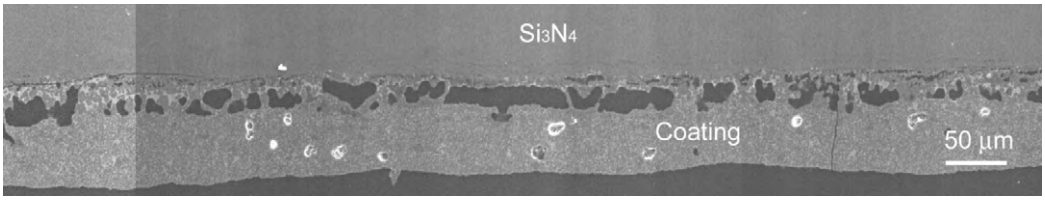

Fig. 6. SEM cross-sectional view (montage) of intermediate melting point mullite/Gd_2SiO_5 (88/12 wt.%) slurry coatings on Y_2O_3/Al_2O_3 Si_3N_4 doped Si_3N_4 coupon air sintered at 1400 °C for 3 h followed by thermal cycling between 1350 °C and RT for 100 h. Thermal cycling formed hairline cracks along substrate/coating interface and large, elongated and interconnected pores adjacent to interface causing coating spallation.

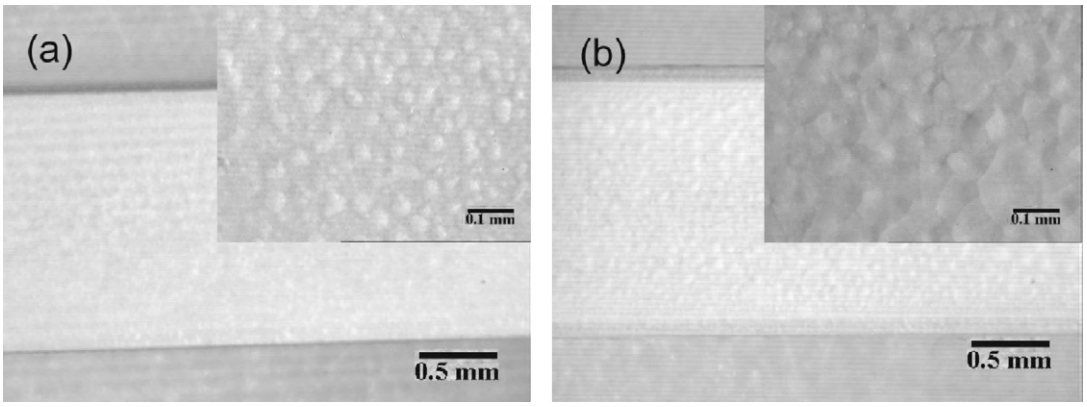

Fig. 7. Optical images of pre-oxidized Si_3N_4 coupons in air at (a) 1300 °C and (b) 1400 °C for 5 h, respectively followed by mullite/Gd_2SiO_5 (88/12 wt.%) slurry coatings and sintered at 1375 °C for 3 h, revealing extensive bubbles on coating due to lowered melting point eutectic formation.

does not appear to have interconnected pores, moisture would not be expected to permeate through the dense EBC. It is likely that the CTE-mismatch induced longitudinal hair-line cracks at the interface provide the lateral pathway for the ingress of moisture to the Si_3N_4.

3.3. Role of yttria-alumina additives in developing slurry based coatings for Si_3N_4

A silica layer forms at substrate/coating interface during air sintering of slurry coated Si_3N_4 coupons. Its thickness depends upon the sintering temperature and time. The yttria-alumina additives already present in the Si_3N_4 react with this silica layer forming a lower melting point eutectic [26]. It is this low melting glassy phase which provides the desired enhanced sintering of the EBC. However, it comes at an expense. The nitrogen oxide, which also forms during air sintering of Si_3N_4, gets trapped below this low viscosity glassy phase generating extensive bubbles, and coat lift-off. This adverse role of yttria-alumina additive is further confirmed by the following observations.

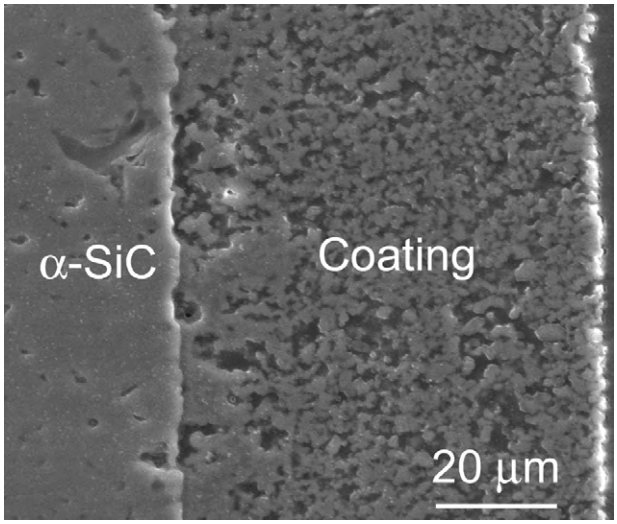

Fig. 8. SEM cross-sectional image of α-SiC coupon coated with mullite powder/mullite sol (50/50 wt.%) slurry and air sintered to 1500 °C for 3 h, which shows good coating adherence to the substrate without any bubble formation even after 1500 °C air exposure.

(a) The Si_3N_4 coupons were pre-oxidized in air for 5 h, one at 1300 °C and the other at 1400 °C, before being coated with mullite/Gd_2SiO_5 (88/12 wt.%) slurry. The pre-oxidization of Si_3N_4 coupons prior to coating results in a silica layer on the sample. It is expected that this enhanced silica content when reacted with yttria-alumina additives would create even lower melting point constituents at the interface, as compared with the non-pre-oxidized Si_3N_4 samples. This was experimentally observed in this study. Fig. 7(a) and (b), respectively, shows surface morphology of the 1300 °C and 1400 °C pre-oxidized Si_3N_4 coupons after they were slurry coated and sintered in air at 1375 °C for 3 h. There was extensive bubble formation below the coating for both these samples; this is more clearly indicated in the higher magnification inset views. The sample pre-oxidized at 1400 °C (Fig. 7(b)) had larger bubbles and more severe bubble formation than the one pre-oxidized at 1300 °C (Fig. 7(a)). In contrast the non-pre-oxidized samples coated with the same slurry did not show such bubble formation when sintered at 1400 °C (Fig. 3(a)). The pre-oxide silica-rich yttria-alumina layer reacts with the Gd_2SiO_5 in the slurry and forms the low melting point constituent which promotes such bubble formation. The higher silica content at the 1400 °C pre-oxidized sample surface, results in an even lower melting point silica-yttria-alumina-Gd_2SiO_5 layer during subsequent sintering, resulting in the more severe bubble formation seen in Fig. 7(b) than that in Fig. 7(a).

(b) As described above, the yttria-alumina containing Si_3N_4 coupons coated with mullite powder/mullite sol (50/50 wt.%) slurry showed extensive bubble formation and coat de-bonding after air sintering at 1430 °C (Fig. 7(b)). However, the same slurry when coated on α-SiC coupon did not show such bubble formation after sintering at much higher temperatures. As shown in Fig. 8, the same mullite powder/mullite sol (50/50 wt.%) coating is well-bonded to the α-SiC substrate, without any indication of bubble formation even after 1500 °C air sintering for 3 h.

4. Concluding remarks

Rare earth silicates with mullite are attractive EBC candidates due to their phase stabilities and lower volatility at high temperatures [19]. However, this study shows that the Y_2O_3/Al_2O_3 dopants, used as sintering additives in Si_3N_4, are serious impediment to using the slurry coating process in order to form mullite and mullite-rare earth silicate EBC on this silicon nitride. They limit the maximum sintering temperature which can be used to convert the as deposited EBC into one having no interconnected porosities. They react with silica and rare-earth silicates to form low melting point constituents at the interface, which causes extensive bubble formation and coating delamination during high temperature sintering which is required to densify the as slurry deposited EBC.

References

[1] W.A. Sanders, D.M. Mieskowski, Am. Ceram. Soc. Bull. 64 (2) (1985) 304–309.
[2] A. Tsuge, K. Nishida, Am. Ceram. Soc. Bull. 57 (4) (1978) 424–426.
[3] S. Guo, N. Hirosaki, Y. Yamamoto, T. Nishimura, M. Mitomo, Scripta Mater. 45 (2001) 867–874.
[4] E.J. Opila, R.C. Robinson, D.S. Fox, R.A. Wenglarz, M.K. Ferber, J. Am. Ceram. Soc. 86 (8) (2003) 1262–1271.
[5] M.N. Menon, H.T. Fang, D.C. Wu, M.G. Jenkins, M.K. Ferber, K.L. More, C.R. Hubbard, T.A. Nolan, J. Am. Ceram. Soc. 77 (5) (1994) 1217–1241.
[6] H.T. Lin, P.F. Becher, M.K. Ferber, V. Parthasarathy, Key. Engg. Mat. 161–163 (1999) 671–674.
[7] H.T. Lin, M.K. Ferber, W. Westphal, F. Macri, ASME Turb Expo 2002, Amsterdam, 2002-GT-30629.
[8] H.T. Lin, M.K. Ferber, J. Eur. Ceram. Soc. 22 (2002) 2789–2797.
[9] J.-F. Yang, T. Ohji, K. Niihara, J. Am. Ceram. Soc. 83 (8) (2004) 2094–2096.
[10] E.Y. Sun, P.F. Becher, K.P. Plucknett, C.-H. Hsueh, K.B. Alexander, S.B. Waters, K. Hirao, M.E. Brito, J. Am. Ceram. Soc. 81 (11) (2005) 2831–2840.
[11] H. Klemm, C. Taut, G. Wotting, J. Eur. Ceram. Soc. 23 (2003) 619–627.
[12] N.S. Jacobson, J. Am. Ceram. Soc. 76 (1) (1993) 3–28.
[13] J.L. Smialek, R.C. Robinson, E.J. Opila, D.S. Fox, N.S. Jacobson, Adv. Compos. Mater. 8 (1) (1999) 33–45.
[14] D.S. Fox, E.J. Opila, Q.N. Nguyen, D.L. Humphrey, S.M. Lewton, J. Am. Ceram. Soc. 86 (8) (2003) 1256–1261.
[15] E.J. Opila, R.E. Hann Jr., J. Am. Ceram. Soc. 80 (1) (1997) 197–205.
[16] E.J. Opila, D.S. Fox, N.S. Jacobson, J. Am. Ceram. Soc. 18 (4) (1997) 1009–1012.
[17] V.K. Pujari, U.S. Patent 6,682,820 B1 (2004).
[18] K.N. Lee, R.A. Miller, Surf. Coat. Technol. 86–87 (1996) 142–148.
[19] K.N. Lee, D.S. Fox, N.P. Bansal, J. Eur. Ceram. Soc. 25 (2005) 1705–1715.
[20] I. Tsarenko, H. Du, W.Y. Lee, J. Am. Ceram. Soc. 87 (3) (2004) 417–420.
[21] W.Y. Lee, K.L. More, D.P. Stinton, Y.W. Bae, J. Am. Ceram. Soc. 79 (9) (1996) 2489–2492.
[22] T. Bhatia, H. Eaton, J. Holowszak, E. Sun, V. Vendula, DOE EBC Workshop, Nashville, Nov. 18 (2003).
[23] I. Tsarenko, S. Park, H. Du, W.Y. Lee, J. Am. Ceram. Soc. 86 (9) (2003) 1622–1624.
[24] B.L. Armstrong, K.M. Cooley, J.A. Haynes, H.-T. Lin, Environmental Barrier Coatings Workshop, Nashville, Nov. 6 (2002).
[25] T. Suetsuna, M. Ishizaki, M. Ando, N. Kondo, T. Ohji, S. Kanzaki, J. Ceram. Soc. Jpn. 112 (5) (2004) 301–304.
[26] M.J. Hyatt, D.E. Day, J. Am. Ceram. Soc. 70 (10) (1987) C-283–287.
[27] K.N. Lee, US Patent, US 2009/0186237 A1.
[28] S. Ueno, D.D. Jayaseelan, T. Ohji, H.T. Lin, J. Ceram. Proc. Res. 6 (1) (2005) 81–84.
[29] G.F. Chen, K.N. Lee, S.N. Tewari, J. Ceram. Proc. Res. 8 (2) (2007) 142–144.
[30] R. Sivakumar, S.N. Tewari, D.S. Fox, K.N. Lee, R.T. Bhatt, Surf. Coat. Tech., in press.
[31] R. Sivakumar, S.N. Tewari, D.S. Fox, K.N. Lee, R.T. Bhatt, Surf. Coat. Tech., submitted for publication.
[32] K.N. Lee, D.S. Fox, J.I. Elridge, D. Zhu, R.C. Robinson, N.P. Bansal, R.A. Miller, J. Am. Ceram. Soc. 86 (8) (2003) 1299–1306.